COMMISSION OF THE EUROPEAN COMMUNITIES

JOINT RESEARCH CENTRE

ISPRA ESTABLISHMENT

NEWSLETTER
12

TELLUS PROJECT

TELLUS - NEWSLETTER 12 January 1980

IMAGE PROCESSING OF HCMM-SATELLITE THERMAL IMAGES FOR SUPERPOSITION WITH OTHER SATELLITE IMAGERY AND TOPOGRAPHIC AND THEMATIC MAPS*

by: *H. Gossmann*
Geographisches Institut I der Universität Freiburg
D-7800 Freiburg
and
P. Haberäcker
DFVLR, Institut für Nachrichtentechnik,
D- 8031 Oberpfaffenhofen

* This research is financially supported by the " Deutsche Forschungsgemeinschaft".
The authors are grateful to:
H.- J. Böhnel, Institut für Physikalische Weltraumforschung
W. Endlicher
W. Nübler Geographisches Institut I der Universität Freiburg
W. Weischet
for their helpful discussions in preparing this paper.

Correspondence regarding this series of newsletters should be addressed to :
P. REINIGER Commission of the European Communities
JOINT RESEARCH CENTRE
I-21020 Ispra (Varese) - Italy

Image processing of HCMM-satellite thermal images for superposition with other satellite imagery and topographic and thematic maps

Abstract

Heat Capacity Mapping Mission (HCMM) is the first of a series of low-cost, modular-design space craft built for the Applications Explorer Missions (AEM). This mission was designed to allow scientists to determine the feasibility of using day-night thermal infrared remote sensor-derived data. HCMM was launched on April 26, 1978, into a nearly sun-synchronous 620 km circular orbit inclined 97.6 degrees to the equator. The selected orbit has a 16-day repeat cycle. The HCMM carries a single sensor called HCMR (Heat Capacity Mapping Radiometer) which is a two-channel scanning radiometer providing measurements of reflected solar and emitted thermal energy. Under the leadership of the Joint Research Centre of the European Communities in Ispra (Northern Italy) a consortium of several European investigators conducts studies of soil moisture and heat budget evaluation of HCMM-data in selected European Zones of agricultural and environmental interest (TELLUS-Project). The objectives of this paper are: How exact a regionally bounded HCMM-scene can be rectified with respect to a preassigned coordinate system. Related to this problem is the question of the scale to which excerpts from HCMM-data can be sensibly enlarged or how large natural topographic structures must be in order to identify them in a satellite thermal image with the given resolution.
Furthermore, an attempt will be made to superimpose within the computer the HCMM-data with other information , especially relief and forest and population distribution maps, but also with a land-use map, which has been derived from LANDSAT data. Here it is necessary to digitalize the maps and to adapt them to a common reference system and to combine the various information levels in a single multi-channel data-structure. As area under investigation a section has been chosen from the southwestern part of Central Europe between the cities Basel and Frankfurt. This section comprises the Upper Rhine Valley and the surrounding highlands. The digitalization of the maps was achieved after a photographically preprocessing by scanning 6 x 6 cm^2 slides with a flying-spot-scanner of the DIBIAS-system, which was the digital image processing system used for the described work. After the digitalization, all maps have been fitted to the reference system and in this way to each other. For the geometrical rectification of the maps and the original HCMM data the interpolation method with control points for the calculation of the parameters of the mapping functions have been used. In order to achieve the highest possible degree of precision the determination of the control points has been carried out in two steps. First, the thermal-image has been corrected with respect to the water network and the forest distribution. From the thermal image treated in this way - and which already approaches in its geometry the topographical map - the control points for the rectification have been determined using the coordinates of the reference system. The final rectification yielded a r.m.s. error of about one pixel (618 m and 408 m). After the geometrical rectification the several information channels have been merged to one multi-channel scene which could be evaluated in several different manners, like the correlation of surface temperature and relief, surface temperature and land-use and surface temperature and built-up areas.

Table of contents

Image processing of HCMM-satellite thermal images for superposition with other satellite imagery and topographic and thematic maps

1. Introduction

1.1 Heat Capacity Mapping Mission (HCMM)

HCMM is the first of a series of low-cost, modular-design spacecraft built for the Applications Explorer Missions (AEM). This mission was designed to allow scientists to determine the feasibility of using day-night thermal infrared remote sensor-derived data for [1]:

- Discrimination of rock types and mineral resource locations.
- Measuring soil moisture effects by observing the temperature cycle of soils.
- Measuring plant canopy temperatures at frequent intervals to determine the transpiration of water and plant stress.
- Utilizing frequent coverage of snow fields for water runoff prediction.
- Measuring effects of urban heat islands.
- Mapping surface thermal gradients on land and in water bodies.

HCMM was launched on April 26, 1978, into a nearly sun-synchronous 620 km circular orbit inclined 97.6 degrees (retrograde) to the equator. At northern hemisphere mid-latitudes, the crossing times are about 1 : 30 p.m and 2:30 a.m. The selected orbit has a 16-day repeat cycle. This orbit results in satellite night/day coverage patterns at least once every 16 days at approximately 12-hour intervals for all latitudes poleward of 35 degrees, and all latitudes equatorward of 20 degrees.

The HCMM carries a single sensor called HCMR (Heat Capacity Mapping Radiometer). This instrument is a two-channel scanning radiometer providing measurements of reflected solar and emitted thermal energy. Fig. 1 summarizes the major characteristics of the HCMR:

Orbital altitude	=	620 kilometers
Angular resolution	=	0.83 milliradians
Resolution	=	0.6 km x 0.6 km at nadir (infrared) 0.5 km x 0.5 km at nadir (visible)
Swath width	=	716 kilometers
Thermal channel	=	10.5 to 12.5 micrometers NEDT = 0.4 K at 280 K
Usable range	=	260 to 340 K
Visible channel	=	0.55 to 1.1 micrometers
Dynamic range	=	0 to 100 % albedo

Fig. 1: Heat Capacity Mapping Radiometer Summary Data Sheet

NASA had some problems with the calibration of the thermal data since after launch of the HCMM some instrument characteristics changed slightly for unknown reasons. Consequenly HCMM surface-temperatures in this paper have been provisionally calibrated and one might have to correct them later.

NASA had planned a mission-duration of one year. Information concerning the data available up to now will be given in section 2.3.

1.2 TELLUS-Project

Under the leadership of the Joint Research Centre of the European Communities in Ispra (Northern Italy) a consortium of several European investigators conducts studies of soil moisture and heat budget evaluation of HCMM-data in selected European zones of agricultural and environmental interest (TELLUS-Project).

Anticipated results are:

- Seasonal mapping of soil moisture;
- monitoring of vegetation stress;
- relationships between soil moisture, groundwater and erosion;
- frost tendency monitoring and
- effect of heat sources and sinks on regional heat budget.

Some special interests of the Geographical Institute I of the University of Freiburg (GEOIF) in the frame of TELLUS-Project are [2]:

- Connection between the patterns of surface temperatures, respectively day/night temperature differences and the geographic reality of various natural surfaces with a different physical constitution (forests, farmland, settling areas etc.) by comparison with already available special maps mainly in the scale 1 : 1,000,000.

- Correlation between surface temperatures or their variations and the nature of surface coverage.

- Analysis of the influence of altitude, topographic situation and regional meteorologic conditions on the temperature of surface elements of the same kind.

- Thermal behaviour of different regional units in Southern Germany.

1.3 Objectives

In this paper two questions, both of primary importance for the application of HCMM-image material with regard to the above-mentioned goals, will be examined.

It will be examined, how exact a regionally bounded HCMM-scene can be rectified with respect to a preassigned coordinate system (in this case the Gauss-Krüger System for the official maps of the Federal Republic of Germany). Related to this problem is the question of the scale to which excerpts from HCMM-data can be sen-

sibly enlarged or, conversely, how large natural topographic structures must be in order to be identified accurately in a satellite thermal image. This information is a prerequisite for all evaluations in which HCMM data are related to terrestrial observations or measurements.

Furthermore, an attempt will be made to superimpose computationally point for point the HCMM-image data with other informations, especially relief and forest and population distribution maps, but also with a land-use map, which has been derived from LANDSAT data. Here it is necessary, on the one hand, to digitize the maps and to rectify them, likewise with respect to the Gauss-Krüger coordinate system, and, on the other hand, to combine the various information levels in a single multi-channel data-structure. The thereby requisite methodological steps and the accompanying difficulties, as well as some evaluations of the resultant data-structures, will be presented below.

1.4 The area under investigation

For this study a section has been chosen from the southwestern part of Central Europe between the cities of Basel and Frankfurt (Fig. 2). This section comprises the so-called Upper Rhine Valley and the surrounding Highlands. There are several reasons for this choice:

Both sides of the Rhine river are exemplified by a variety of landscape types: the holocene flood plain with residual forests; the intensely cultivated quarternary accumulation plain, interspersed in some places with forested sand and gravel terrain; the orchards and vineyards of the foothill zone; the strongly dissected forested ascent to the mountainous flanks of the Graben; forested plateaus, extending away from the Upper Rhine Valley and divided by large valleys, and which on the side away from the Rhine are bounded by a wellmarked rock formation and thereafter replaced by a relatively unforested farm landscape.

On the Upper Rhine Valley there are several very densely populated regions, like Frankfurt and Mannheim-Ludwigshafen in the Federal Republic of Germany, Strasbourg in France, and Basel in Switzerland. Outside of these centres with their great need for space, a strong industrial development is taking place, especially along the Rhine river on the German and even more so on the French side, a development which in this area has led to an active discussion about the possibilities of a man-made modification of the regional heat-budget [3].

Flights carried out in 1976 by the German Aerial Surveying Program have made available day and night thermal-images for several sections of the area in question. These images can be combined with HCMM data [2].

As the result of a study on the evaluation of LANDSAT data for the preparation of land-use data to be used in regional planning there is already available a digital map of the Mannheim area with the territory classified into eight land-use classes. This allows a direct combination with HCMM data [4].

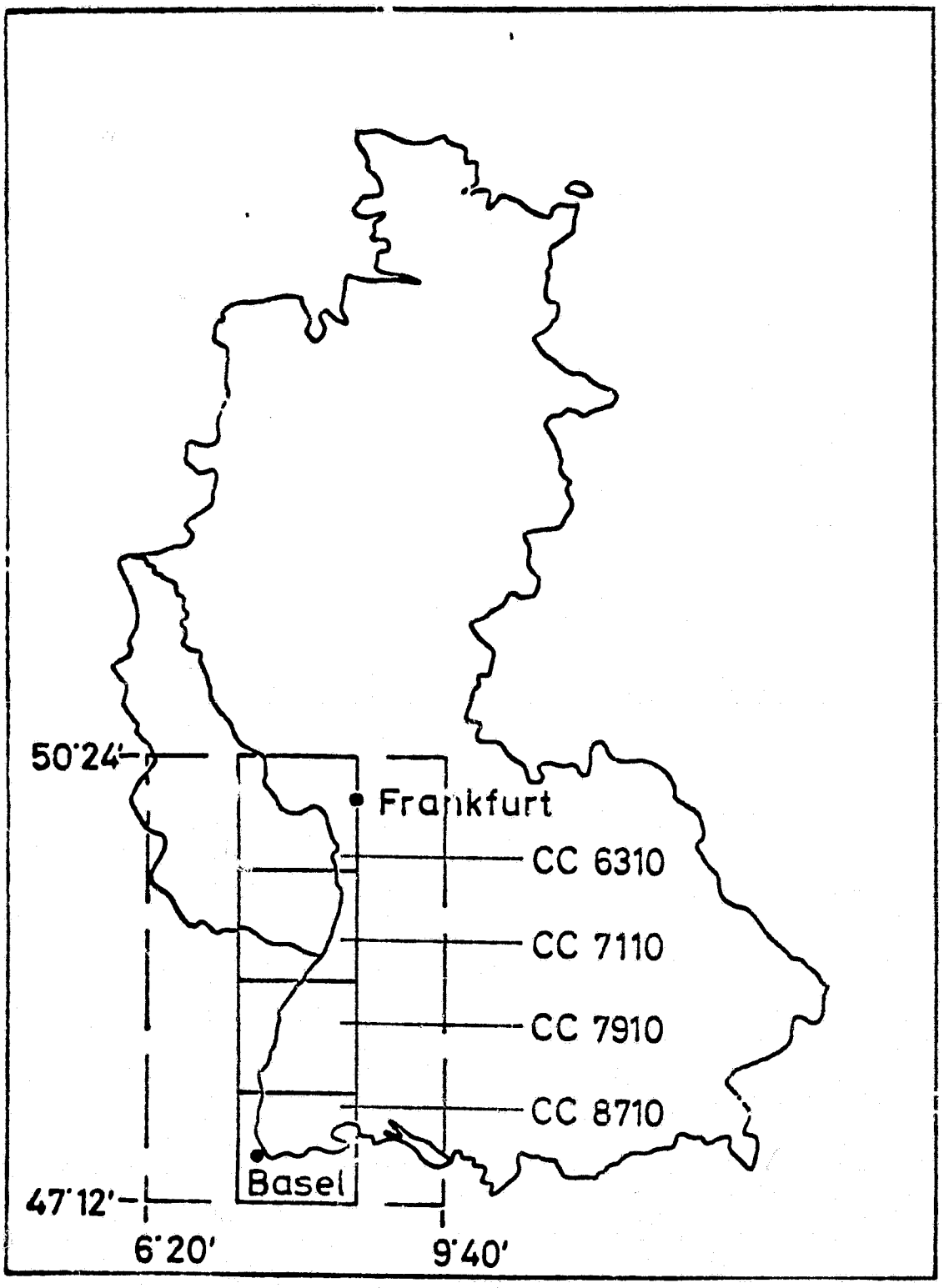

Fig. 2: The area under investigation
CC 6310, CC 7110, CC 7910 and CC 8710 are sheet-numbers of the official Topographical Map 1 : 200,000 of the FRG.

In the following, the area in question will be considered as a whole as well as in some of its parts. These parts correspond to the sheets of the official maps of the Federal Republic of Germany, scale 1 : 200,000 (TÜK 200; Fig. 2).

2. Data Base

2.1 Maps

Of all the types of existing thematic maps showing distribution patterns of specific phenomena, two are of special interest with regard to superimposing with satellite images. The first type is the distribution pattern of land-use types, in which the illustrated area is composed of "sub-surfaces", each class of sub-surface representing a particular geographic quality, as is the case with land-use maps. The binary distribution maps of a land-use category (binary mosaic map), such as those for forest distribution or the distribution of tilled or settled acreage in a given area, are special cases of this type. The second map-type is comprised of the iso-line representation of a continuum, i.e., of a continuous field which fills the observed area, as e.g. the contour representation of land forms. On the other hand, maps constructed on the basis of a network of linear elements, such as the network of rivers, streams, lakes, etc., of an area, can only be used for orientation purposes or as a frame of reference, since, because of the extraordinary broadness of the line, the image-elements which appear on the map as bodies of water must not necessarily represent water in the satellite image, too.

One example of each of these two map-types has been selected for investigation (Fig. 3a). In choosing an appropriate scale the geometric resolution of the satellite thermal-image was the decisive factor. Assuming the smallest possible size of the map-elements to be 0.3 mm x 0.3 mm, the pixel size of 600 m x 600 m corresponds to a scale of 1 : 2,000,000. Therefore, in the digitalization (cf. 3.1) maps of the scale 1 : 1,000,000 and 1 : 2,000,000 have been employed. The originals have been taken in part from the atlas "Bundesrepublik Deutschland in Karten", in part they are working-copies from the "Hydrologischen Atlas der BRD". Fig. 3b shows as an example the forest distribution map which has been used in this study. The relevant sheets of the Topographical Map of Federal Republic of Germany, scale 1 : 2,000,000 (TÜK 200, Fig. 2), served as the basis for the geometric rectification and the fitting of the entire data-structure to the Gauss-Krüger Coordinate System.

Contents	Type	Scale	Source
Relief	contour map	1:2,000,000	Hydrologischer Atlas der FRG
Forest distribution	binary mosaic map	1:2,000,000	Hydrologischer Atlas der FRG
Urban built-up areas	binary mosaic map	1:1,000,000	FRG in Karten
Water	network of linear elements	1:2,000,000	Hydrologischer Atlas der FRG

Fig. 3a: Overview of the thematic maps which have been digitized and with which thermal images have been superimposed.

2.2 LANDSAT image sources

As above mentioned LANDSAT image data were used as a further data base. These data were produced in connection with an investigation of the application-possiblities of satellite-image data in the regional planning sector [4]. Specifically, the data sources are two LANDSAT scenes of southwestern Germany, the one dated 8/9/1975, the other 8/28/1975, both of which were geometrically rectified and adapted to the Gauss-Krüger coordinate system. Segments of both scenes have been fitted together so as to form a mosaic which covers the map CC 7110 (Mannheim, scale 1:200,000). Each pixel of the rectified and CC 7110-fitted scenes describes a surface of 100 x 100 m^2 (1 ha). The following 8 classes were established by multispectral classification: high-density urban built-up, low density urban built-up, water, pastures and orchards, tilled acreage, vineyards, deciduous forest and coniferous forest. The so classified scene is available as a data-structure which can be combined with other data sources. Fig. 14 demonstrates the combination of the classified scene with the information of the topographical map for the same region. In the present investigation the combination was carried out using the infrared data of the HCMM satellite (cf. sections 5 and 6 of this paper).

2.3 The HCMM scene

Although the HCMM satellite has been operating for a year, there is at the moment (June 1979) only one image available for evaluation, namely from May 30, 1978, 2:13 GMT (Fig. 6). This is because, firstly, the high degree of cloud coverage over Central Europe renders many images unusable and, secondly, due to scheduling conflicts with other NASA programs, the European ground stations in Madrid and elsewhere could not register data during the clear-weather period of October 1978.

On the other hand it has not been a disadvantage that the studies on combining thermal information with the afore-mentioned informa-

tions have had to be centered up until now on a single image. As soon as they are available, new images can be integrated easily into the data-structures which have already been produced and can be thus subjected to multi-temporal observation.

Fig. 3b: Forest Distribution in South-West Germany from Hydrologischer Atlas der Bundesrepublik Deutschland.

3. Preparation of auxilary data (map digitalization)

Map digitalization was achieved by scanning 6 x 6 cm^2 slides with a DICOMED-Flying-Spot-Scanner (DIBIAS System). This system allows a resolution of the image in 1024 x 1024 pixels. Considering the extension of the Upper Rhine Valley and its surroundings this result in a pixel size of ca. 350 x 350 m^2 (cf. Fig. 2). This resolution corresponds approximately to the accuracy of the map: 350 m ≙ 0.35 mm and 0.175 mm in scales of 1:1,000,000 and 1:2,000,000, respectively. At the same time it is somewhat better than the geometric resolution of the thermal-image.

The digitizing of gray levels which appear on the maps presented considerable difficulties. It proved to be impossible to carry out the digitalization of a gray tone scale with more than two levels in one step. Furthermore, because of vignetting effects the binary black and white prints also show a strong distortion of the image contents. Using the relief map as an example, the solution to this problem is described below.

When it became apparent that the separation of the gray values for the digitalization of the five elevations on the relief map would not be possible using the available apparatus, the elevations were removed one by one from the original map according to the strip mask procedure *). They are thus represented on the film by black patches. These five photos, to which scanning markers were added, as well as a sixth transparency which contains only scanningmarkers, are designated I_1, I_2, I_3, I_4, I_5 and T corresponding to the following legend:

I_1	0 - 200 m
I_2	200 - 400 m
I_3	400 - 700 m
I_4	700 - 1000 m
I_5	> 1000 m
T	scanning markers only

In the digitalization the most exact coordination of the five images that was possible was achieved by careful adjustment of each image on the scanning frame, using a magnifying glass and the pass markers. The numerical fields (matrices) thus produced are called I_1', I_2', I_3', I_4', I_5', and T'. The superimposition of any two of the I_i in the interactive colour monitor (COMTAL) of the DIBIAS-system showed that because of smaller fitting errors and a little play in the scanning frame of the digitizer, the digitized ele-

---

*) We wish to thank H.J. Paul of the Geographical Institute of the University of Freiburg for help and advice during the preparation and realization of the maps.

vation levels did not completely fit together. The overlaps and gaps which thus arose have been made visible by colour representation and could be corrected by shifting individual images by one to two pixels. The necessary shifts correspond to errors in the scanned images of 1/20 mm and 1/10 mm, respectively.

In this way the five digital elevation-images could be joined together to form a map - provided each were already binary. But this is not the case, since even in the scanning of a black and white print far more than just two gray tones will appear in the digitalized image. This is caused by

- o vignetting effects (shadowing on the edges) during the photographic production of the respective copy I_i,
- o vignetting effects from the digitizing device,
- o eclipse- or illumination-effects at the borders of bright and dark.

Because of vignetting, a white background becomes darker towards the edges of the image, but the black elevation representations are also subject to this distortion (Fig. 4a, b). The threshold, which must be established to produce a binary scene, would therefore be position-dependent. As a corrective measure the digital image T' of the completely white transparency T has been used. Since it was produced under the same conditions as the images I_1', ..., I_5', T' contains the same vignetting-effects (Fig. 4c). By subtracting the gray values of the image T' from those of I_i', one obtains images I_i'' which are free of vignettes. The equation is $I_i'' = I_i' + 180 - T'$ (MM-Module of the DIBIAS-System, [5]). Accordingly, the cross section of the image I_i' which appears in Fig. 4b obtains after correction the shape shown in 4d.

Even after correction of vignetting there remains at the dark-bright-edges a gradual transition from white to black (Fig. 4d). Therefore, for the construction of the binary image in each case a threshold value must be established which ascribes the gray values in the transition zone to either black or white. If this value becomes too large, then fine white structures disappear in the black environment. The opposite occurs if the threshold value is too small. This threshold value (gray value 144) was ascertained interactively on the monitor screen. Finally, every elevation was characterized by a definite gray value according to the statement

$$I_i'' = \begin{cases} g_i & \text{if } I_i'' < 144 \\ 0 & \text{otherwise} \end{cases}$$

with the following values for g_i:

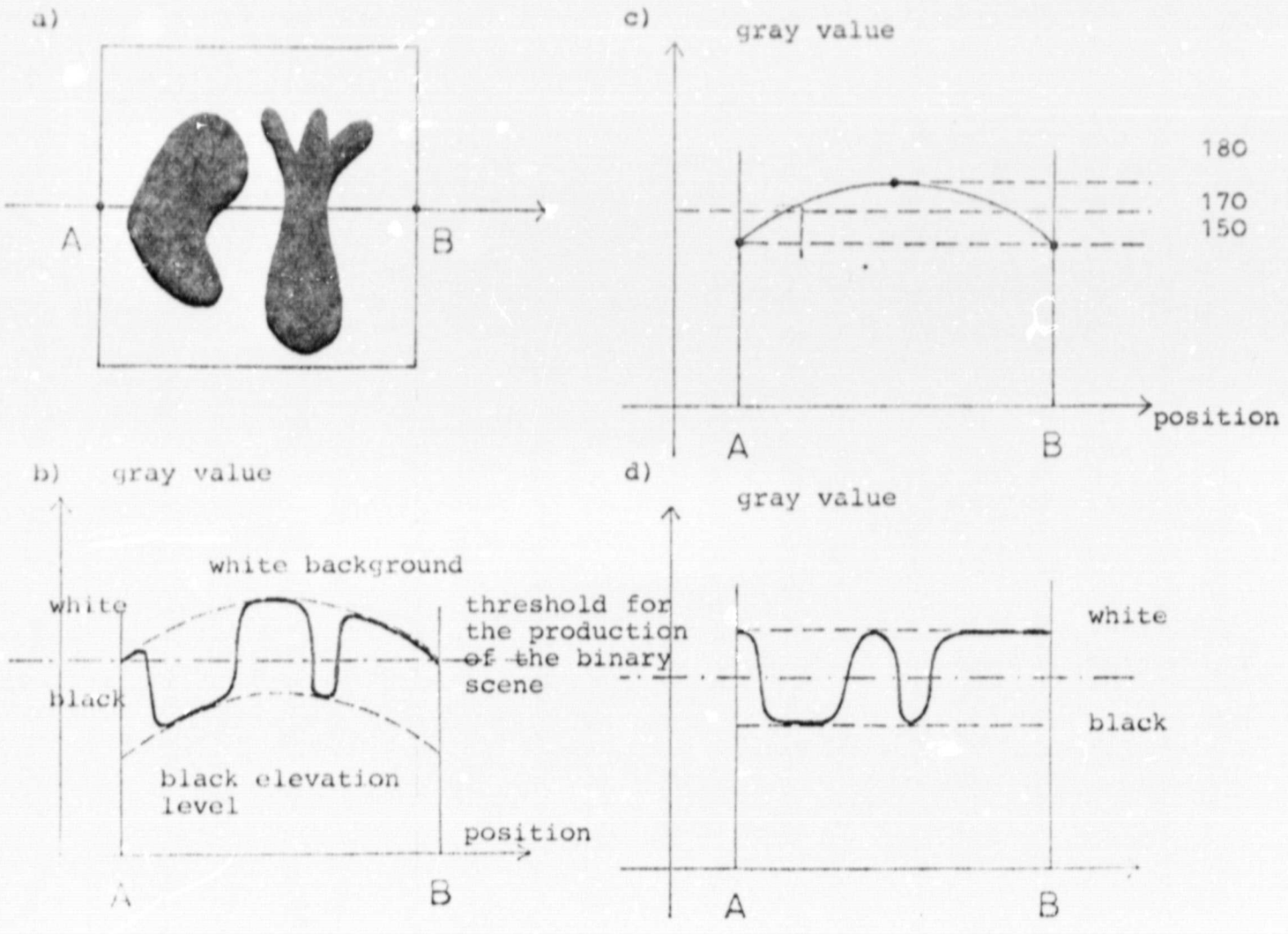

Fig. 4: Sketches representing the suppression of vignetting in digitalized maps prior to the production of a binary scene.

a) Because of position-dependent illumination of the image during the photographic production of the image-copy and during scanning undesired light intensity oscillations become evident in the images I_i'.

b) Profile of section AB from Fig. 4a in the case of a typical edge-shadowing.

c) A section in a completely white image ("vignetting-image" T') corresponding to the profile of section AB in Fig. 4a.

d) Result of correction by means of the equation $I_i'' = I_i' + 180 - T'$ (Subtraction of the vignetting-image from the respective scene and shift of the values into a region of medium gray tones).

Image	Elevation	Characterizing Gray Value g_i
I_1'''	0 - 200 m	230
I_2'''	200 - 400 m	180
I_3'''	400 - 700 m	130
I_4'''	700 - 1000 m	80
I_5'''	> 1000 m	30

Following this preparation the five individual images have been merged by the ME-module [5] into a five-channel image and then assembled by the MM-module [5] according to the following formula to form a relief map with the five elevations in one channel:

```
R = (K1 NE 0) *(K2 EQ 0) *(K3 EQ 0) *(K4 EQ 0) *(K5 EQ 0)* K1 +
    (K1 EQ 0) *(K2 NE 0) *(K3 EQ 0) *(K4 EQ 0) *(K5 EQ 0)* K2 +
    (K1 EQ 0) *(K2 EQ 0) *(K3 NE 0) *(K4 EQ 0) *(K5 EQ 0)* K3 +
    (K1 EQ 0) *(K2 EQ 0) *(K3 EQ 0) *(K4 NE 0) *(K5 EQ 0)* K4 +
    (K1 EQ 0) *(K2 EQ 0) *(K3 EQ 0) *(K4 EQ 0) *(K5 NE 0)* K5.
```

The relief maps which are produced in this way still show gaps (gray value = 0) at the borders between adjoining elevations. These arise during the removal of the elevations from the original map, because with the stripmask procedure the contour lines themselves are not reproduced, i.e., the lines are attributed to neither of the adjoining elevations. The gaps were divided equally between adjoining elevations by means of a special extension operator of the DIBIAS-system (BS-module, [5]).

The maps representing the distribution of forests, built-up areas and rivers were digitized similarly. Special mention must be made of the type of vignetting-effect in the distribution map of built-up areas and the corresponding correction procedure. Here the vignetting consisted in a darkening tendency which ran diagonally in a swath across the image increasing gradually from lower left to upper right. The decrement of the gray-value of white surfaces of 25 points from the lower left to the upper right corner has been ascertained by means of microdensitometric sections parallel to the diagonal. By addition of a correction term the gray-values have been standardized in the following equation, thus:

$$GR_{new} = GR_{old} + (ZE - SP) \cdot 25/ZZ$$

GR = gray-value, ZE = line number, SP = column number

ZZ = number of lines in the image.

After digitizing all maps were fitted to the Gauss-Krüger coordinate system and in this way to each other. This occurred according to the same procedure which was used to rectify the thermal-image and which will therefore be described in detail in section 4 of this paper. Finally, with the corner points having been given in Gauss-Krüger coordinates, similar "windows" were cut from the individual maps and digitally superimposed; this served as a quality control of the processing procedure. Fig. 5 shows the relief map superimposed with the urban built-up distribution and water network which were produced in this way (the former represents only the German part of the territory investigated.

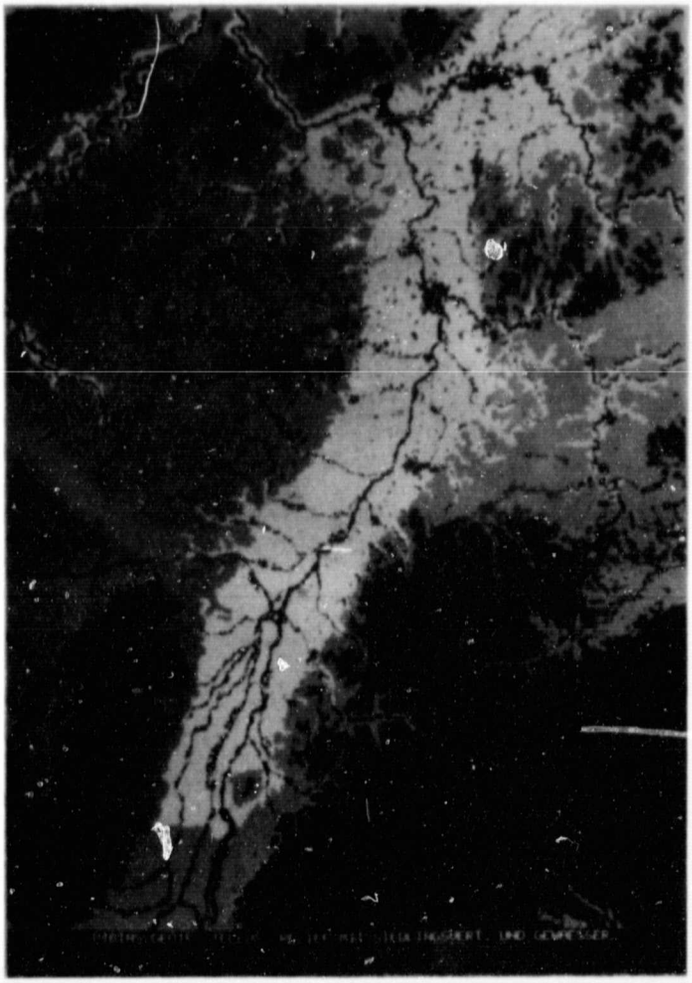

Fig. 5: Result of the digitalization of different maps. Superposition of the relief with the distribution-pattern of urban built-up areas and the river network.

ORIGINAL PAGE IS
OF POOR QUALITY

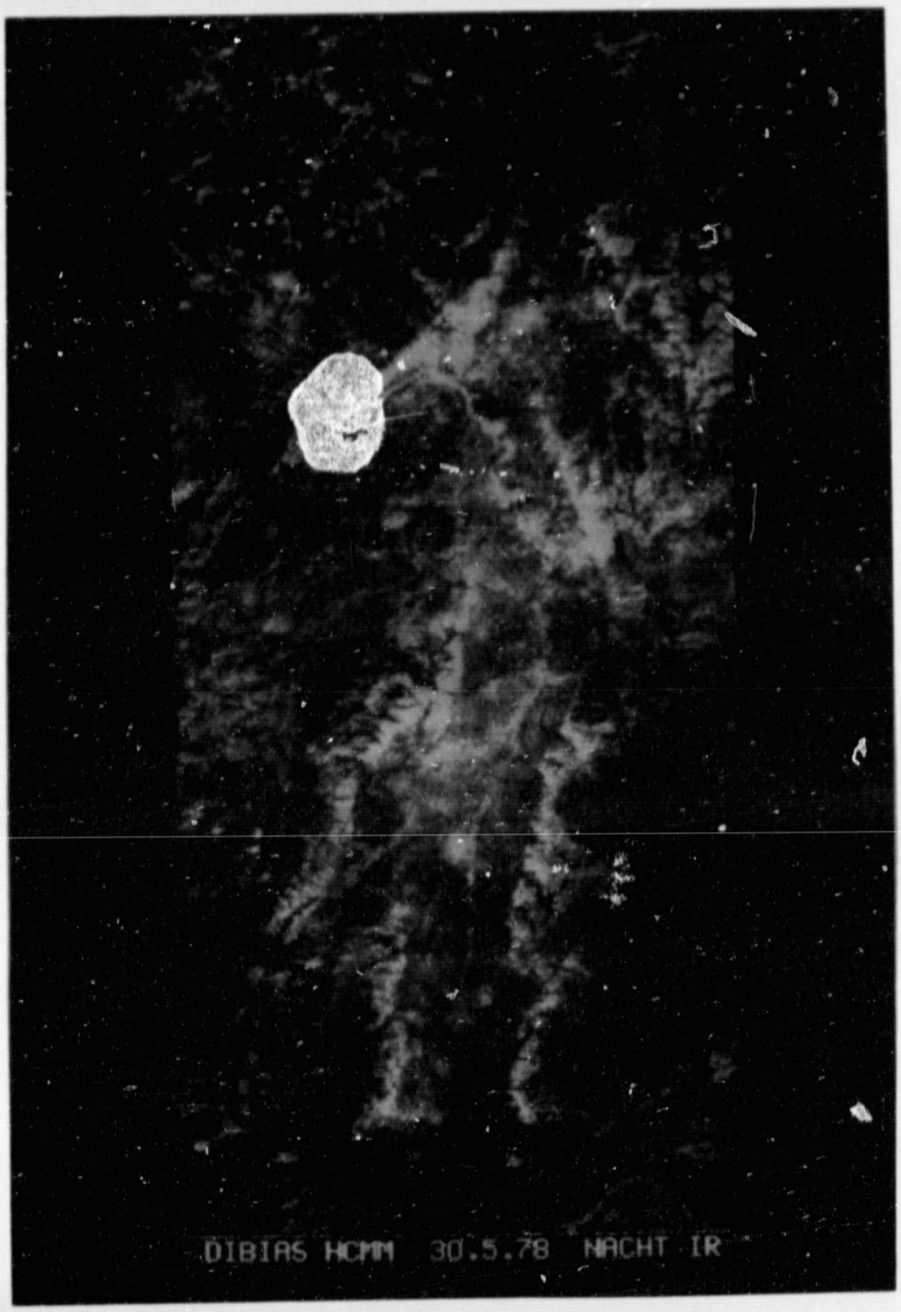

Fig. 6: A section of the thermal infrared HCMM-satellite image (5/30/78, 2:13 GMT). The section shows the Rhine Valley between Basel and Frankfurt and the surrounding highlands (bright ⟶ warm, dark ⟶ cold).

4. Processing the thermal-image

4.1 Geometric adjustment to the Gauss-Krüger coordinate network

4.1.1 Theory

The geometric rectifications in this investigation have been carried out by the interpolation method. This method assumes that between a distorted scene V and a reference-image R there exists a functional dependence

$$R = F\ (V)$$

and that a rectified scene E can be produced by the operation F on V, thus

$$E = F\ (V)$$

The parameters for F are derived from R and V by the control point method, i.e., corresponding control points are sought in the reference-image R and the distorted scene V and their respective coordinates are determined in both coordinate systems. This alignment results in a transformation equation, by which all points of the distorted scene can be related to the reference-image.

The following symbols will be used in the equation below:

V	distorted scene
$\underline{v} = (v_1, v_2)^T$	position-coordinates of the distorted scene
$g_v(v)$	gray-value of the picture-element having these coordinates
R	reference-image
$\underline{r} = (r_1, r_2)^T$	position-coordinates of the reference-image
E	rectified scene
$\underline{x} = (x_1, x_2)^T$	position-coordinates of the rectified scene
$g_E\ (\underline{x})$	gray-value of the pixel having these coordinates

The following relationship between the coordinates of the distorted and rectified scenes has been assumed:

$$v = \underline{f}\ (\underline{x}),\ \text{or}$$

$$v_1 = f_1\ (x_1, x_2)$$

$$v_2 = f_2\ (x_1, x_2)$$

If V is generated from E by means of a projection, then the transformations in x_1 and x_2 are linear (1st-order polynomial):

$$v_1 = A_1 x_1 + A_2 x_2 + A_3$$

$$v_2 = B_1 x_1 + B_2 x_2 + B_3, \text{ or}$$

$$\underline{v} = C \underline{x} + \underline{d}$$

with $C = \begin{pmatrix} A_1 A_2 \\ B_1 B_2 \end{pmatrix}$ and $\underline{d} = (A_3, B_3)^T$

For the rectification of satellite scenes a 2nd-order polynomial is often used instead of the linear equation:

$$v_1 = A_1 x_1 + A_2 x_2 + A_3 + A_4 x_1^2 + A_5 x_1 x_2 + A_6 x_2^2$$

$$v_2 = B_1 x_1 + B_2 x_2 + B_3 + B_4 x_1^2 + B_5 x_1 x_2 + B_6 x_2^2$$

In order to calculate the unknown A_i and B_i the control points are used. The number of control points p must thereby be equal to the number k of unknown parameters which have to be calculated per transformation. With more control points available ($p > k$), the error which appears in the polynomial approximation of the function can be minimized by means of a least squares method.

By the rectification an appropriate coordinate-pair (v_1, v_2) from the distorted scene is connected with the coordinates (x_1, x_2) in the rectified scene in accordance with the above equations. The gray-value of this pixel is calculated from the distorted scene.

4.1.2 Definition of the control points

In order to achieve the highest possible degree of precision the determination of the control points proceeds in two steps. First, the thermal image is corrected with respect to water-networks and forest distribution ("rough" rectification). From this corrected image, which already represents a good geometric approach to the topographical map, the control points for the final rectification are determined using Gauss-Krüger coordinates ("fine" rectification).

The determination of the control points for the first step of rectification has been carried out on the DIBIAS-monitor screen. Here the thermal-image as well as the digitized and pointwise correlated forest distribution and water-network maps were deposited in the image memory of the system. In this way one can rapidly compare the images and easily identify their corresponding structures. As an auxilary aid in the present investigation a relief map was used additionally. Although large-area landscape-structures (the Upper Rhine Valley, Kaiserstuhl, large cities) were easy to recognize in the contrast enhanced thermal-image, the detection of control point pairs remained difficult. It turned out, for example, that in the monitor-screen comparison of structures for the region of the Upper

Rhine Valley no control points - except a few well-marked structures of the Rhine itself - could be determined. The search was easier in the Highlands which surround the plain. Here the valleys with their pastures contrast strongly with the forested mountains and hills. They show a lower surface temperature at night due to differences in the heat budget between pastures and forests and the accumulation of cold air on the valley bottoms. One can therefore define as control points the bends in a valley or the confluences of several valleys. This clear pattern of a valley network in the thermal image is lacking in landscapes with unforested plateaus or only partially forested valley slopes, because here the influences of the relief and vegetation distribution on the surface temperatures run in opposite direction.

Seven of the 17 control points used for the "rough" rectification lie on the Rhine river, 2 on prominent corners of forests, and 8 in the bends of valleys and valley confluences of the Highlands. Of the Rhine control points two or three were produced by the river alone, to some the strip of forest along the river banks was of assistance and in the case of two others on the Middle Rhine the influence of the (relatively warm) Rhine Valley slopes which follow the bends of the river was evident.

As mentioned above the control points for the "fine" rectification were determined using Gauss-Krüger coordinates. In order to achieve an average residual error of less than one pixel in the line as well as in the column-direction, it has been attempted on the basis of the topographical overview map, scale 1:200 000 (TÜK 200), to determine the coordinates for 50 to 100 control points with an error of less than 600 m. This requirement means the determination of these points on the map with an accuracy of 3 mm. For doing this the "rough" rectified images have been projected onto the corresponding map sections. By shifting the maps on a magnetic wall, the structures which correspond to the recognizable patterns in the thermal image, namely, relief, forest distribution, water-network, urban built-ups, were assigned in sub-regions of 20 to 40 km in diameter. Corresponding details of the thermal-image and the map were then identified in these partial regions. It became clear along the way that the control points which have been used in the preliminary rectification could, for the most part, not be identified on the map with the necessary accuracy (3 mm). This is true especially for the control points which were taken from the forest distribution data. The corresponding forest distribution patterns are indeed present on the map TÜK 200, however, the relevant corners and edges could only be defined with precision to about 1 cm. The same is true for the "heat islands" of large cities, which are conspicuous in thermal images and useful in small scale classification. But when blown up they are structureless and have such diffuse edges that it is difficult to assign control points within them. On the other hand the relief provides a good reference system, but not the bends or confluences of the large valleys (as was the case with the "rough" rectification), rather, and especially, the many small forms in the upper parts of the drainage basins. Several control points on the Rhine river could thus be taken over from the "rough" rectification directly.

The 86 detected control points, for which a definition within the afore-mentioned margin of error was possible, are distributed among the different classes according to the following list:

Bodies of water *(5 points): Three well-marked bends in the Rhine river, one in the Mosel river, and a corner of a lake which had a rather conspicuous shape. Many of the river-bends have to be disqualified, since it can not be unequivocally determined whether or not the structure which appears in the thermal image is produced by the river itself or by the adjoining strips of forest.

Urban built-up areas (5 points): Although there exist numerous cities with populations of up to 10.000, which evoke a thermal signal, it was possible only in a few cases (Endingen, Waldshut) to distinguish the respective town centers. In two other cases, however, the corner points of large industrial built-up areas could be determined.

Land-use boundaries (18 points): The determination of land-use boundaries was more difficult than expected. Forest-clearings (2), small wooded expanses (3), forest-edges which jut out into or sharply recede from the adjoining landscape (9), etc., can apparently be identified only when the borders of the pixel coincide with the land-use boundaries. In 4 cases land-use boundaries could be recognized by a prominent corner of a dam on the Rhine.

Relief (51 points): With some reservation one can say that the nightly-appearing pattern of various sorts concavities was the most effective aid in identifying the control points on the map TÜK 200. The valley-network of the highlands thus served, in addition to its application for the "rough" rectification, as reverence for the projection of the thermal-image onto TÜK 200. But essentially important here were the small but numerous forks (31) in the upper valley regions, which could be assigned to a definite image-point. Furthermore, in some places it was possible to define with sufficient accuracy the junctions at which small peripheral valleys combine with major ones (8) as well as larger junctions (3) or bends (3) in the valleys.

It should be noticed that for all defined categories or classes only a few of many geographically equivalent situations were recorded in the thermal-image. This is due to smearing in mixed signatures caused by averaging the temperatures of the different objects which contribute to the pixel. From this point one can derive two consequences:

Firstly the fact of this "smearing" reinforces trust in those control points which were finally selected. Exactly those situations have been captured in which the phenomenon producing the signal was located centrally in the respective pixel. Secondly, it is to be expected that some of the control points which were employed here will not always be useful for the rectification of other images of the same territory, even if they are taken at the same

*It should be kept in mind that the available portion of the thermal image contains no large bodies of water. It is assumed that well defined lake shores would also provide control points for the "fine" rectification.

time of day. This is because due to different arrangement of the pixels, the same geographic phenomenon can be reproduced clearly in one image but less prominent in another one.

4.1.3 Quantitative results and precision of the procedure

With the control points thus defined, the entire scene (linear and quadratic polynominals) as well as different selected parts of it have been rectified with respect to the format of TÜK 200 in several computing runs. The table in Fig. 8a shows that for the "rough" rectification the best results reveal a r.m.s. error of somewhat more than 1 000 m in both the line and column direction, for the "fine" rectification the values are 618 and 606 m in line and 468 and 462 m in the column direction. The insignificant difference between the residual errors of the linear and quadratic approaches - 618 and 468 m vs. 606 and 462 m respectively suggests that, with regard to the size of the investigated area (about 300 x 150 km), the increased time-consumption of the quadratic approach (35 min. calculating time vs. 18 min. for the linear approach) is not yet compensated by the relatively small gain in efficiency.

The r.m.s. errors from the individual rectifications of the three TÜK-plates are with one exception all significantly smaller that one pixel of the original data. The somewhat better values for the plates CC 7910 (Freiburg-North) and CC 8710 (Freiburg-South) can well be attributed to the investigators' long experience with this area, especially by the previous work with aircraft scanner thermal imagery, which facilitates the selection of control points in this region.

The fact that after the linear rectification no more essential systematic distortions are present in the image is shown in the r.m.s. vector diagrams of the individual control points (Fig. 8b, 8c): the vectors in the different parts of the image exhibit no specific tendencies.

This argumentation using r.m.s. errors and vector-diagrams of r.m.s. errors contains a high degree of abstraction and, in addition to that, offers no compelling proof of the quality of a rectification since it would hide, for example, a systematic additive error (translation). Therefore, in Fig. 9 to 11 the results of the rectification will be presented by using images as examples. Figs. 9 and 10 show the entire scene following the preliminary rectification and the section of CC 7110 (Mannheim) following the "fine" rectification, overlaid with the corresponding topographic pattern. Fig. 11a shows the surface-temperature distribution within the city boundaries of Freiburg-im-Breisgau as recorded in a satellite thermal-image and after "fine" rectification with respect to Gauss-Krüger coordinates and "smoothing" of the pixel edges. Fig. 11b is taken from an aircraft scanner thermal image of the same region produced under comparable conditions.

I. "Rough" Rectification

Area	Reference map	control points No. Determination	Solution approach	Size of the pixels Original(m)	Image(m)	r.m.s. x-axis bi	x-axis m	r.m.s. y-axis bi	y-axis m	Calculating Time
entire scene[1]	forest	10 monitor screen	linear	1200	1200	1.5	1800	12.6	15000	
	water, network	10 monitor screen	linear			1.2	1440	2.95	3540	
	relief	10 monitor screen	linear			1.3	1560	1.98	2376	
	1:1,000,000 1:2,000,000	11 monitor screen	linear			0.9	1080	1.1	1320	
entire scene (northern portion)	1:2,000,000	9 monitor screen	linear	600	600	1.8	1080	2.05	1230	
entire scene (southern portion)	1:2,000,000	10 monitor screen	linear	600	600	2.5	1500	1.99	1194	
II. "Fine" Rectification										
entire scene	TÜK 200	50 GK[2]	linear	600	600	1.03	618	0.78	468	18 min.
entire scene	TÜK 200	50 GK	quadratic	600	600	1.01	606	0.77	462	35 min.
CC 7110 (Mannheim)	TÜK 200	14 GK	linear	600	125	1.04	624	0.74	444	13 min.
CC 7910 (Freiburg-North)	TÜK 200	17 GK	linear	600	125	0.98	588	0.66	396	13 min.
CC 8710 (Freiburg-South)	TÜK 200	17 GK	linear	600	125	0.87	522	0.76	456	12 min.

[1] entire scene = Upper Rhine Region with surrounding highlands. [2] GK = Gauss-Krüger coordinates.

Fig. 8a: Numerical results of the geometrical rectification.

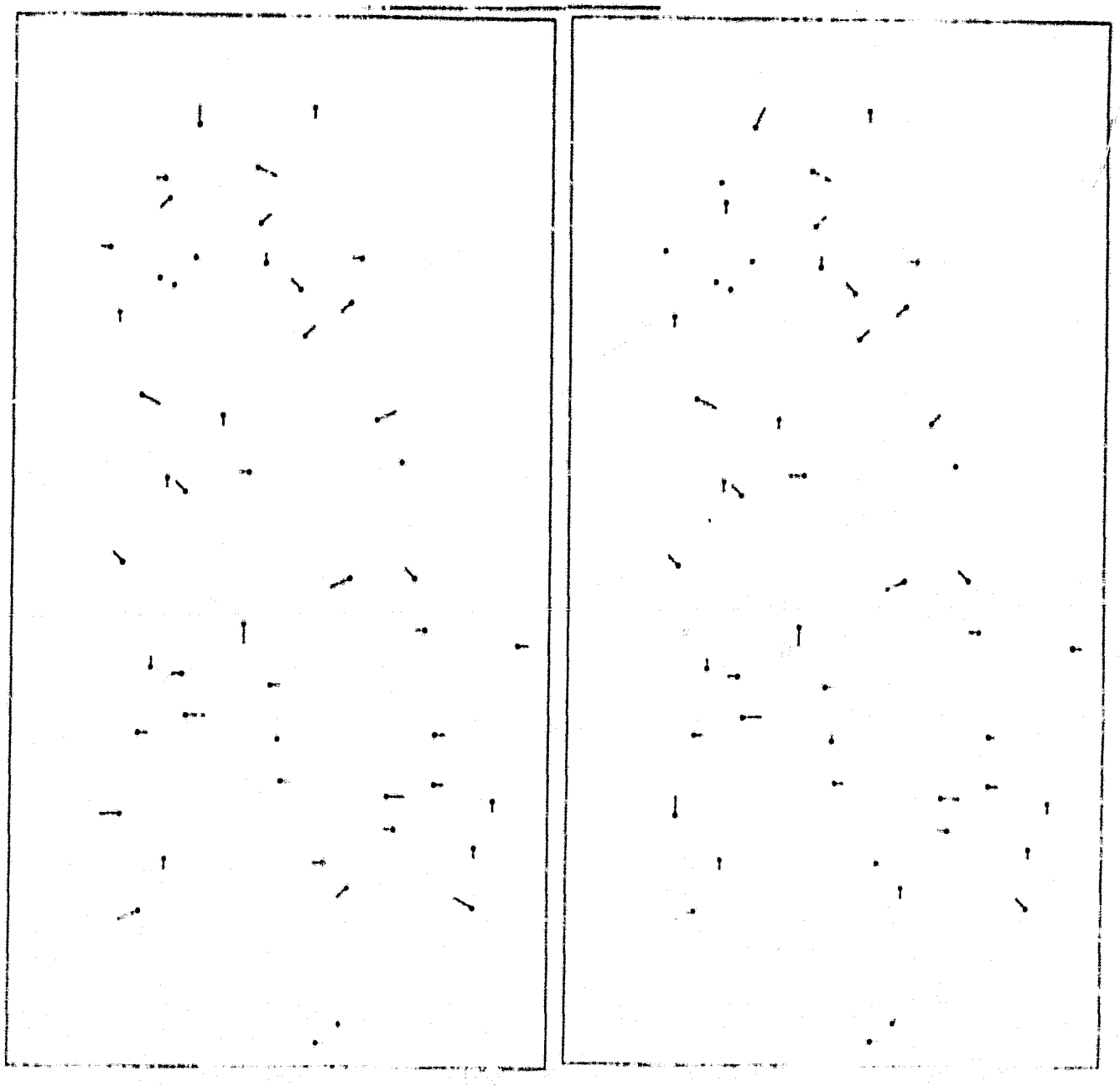

Fig. 8b: Diagram of the r.m.s. vectors in the "fine" rectification of the entire scene; left, quadratic and right linear. For a clear representation the vector length have been stretched by a factor of 8 relative to the scale of the drawings.

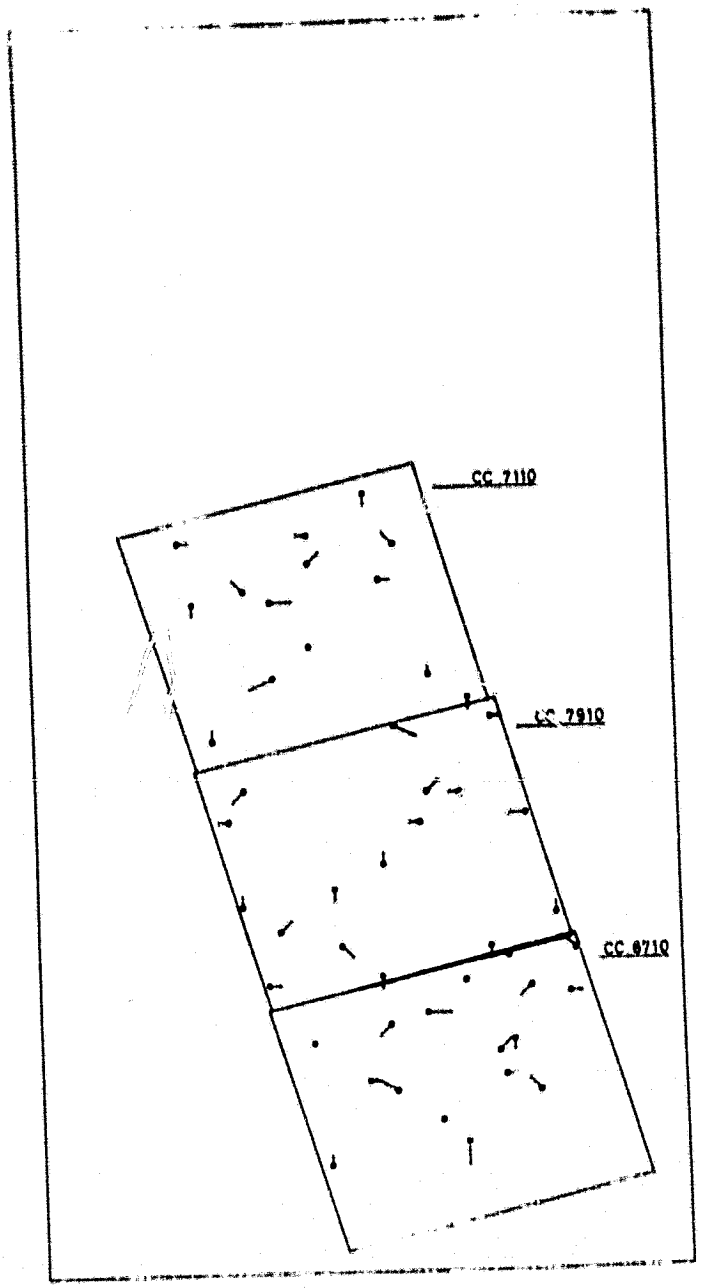

Fig. 8c: Diagram of the residual vectors in the "fine" rectification in accordance with TÜK 200 map plates (cf. the last 3 lines in Fig. 8a). As in Fig. 8b the vector lengths have been increased by a factor of 8.

Fig. 9: Thermal-image (entire scene) after the first step in the rectification ("rough" rectification, line 4 in Fig. 8a). The water-ways are overlaid.

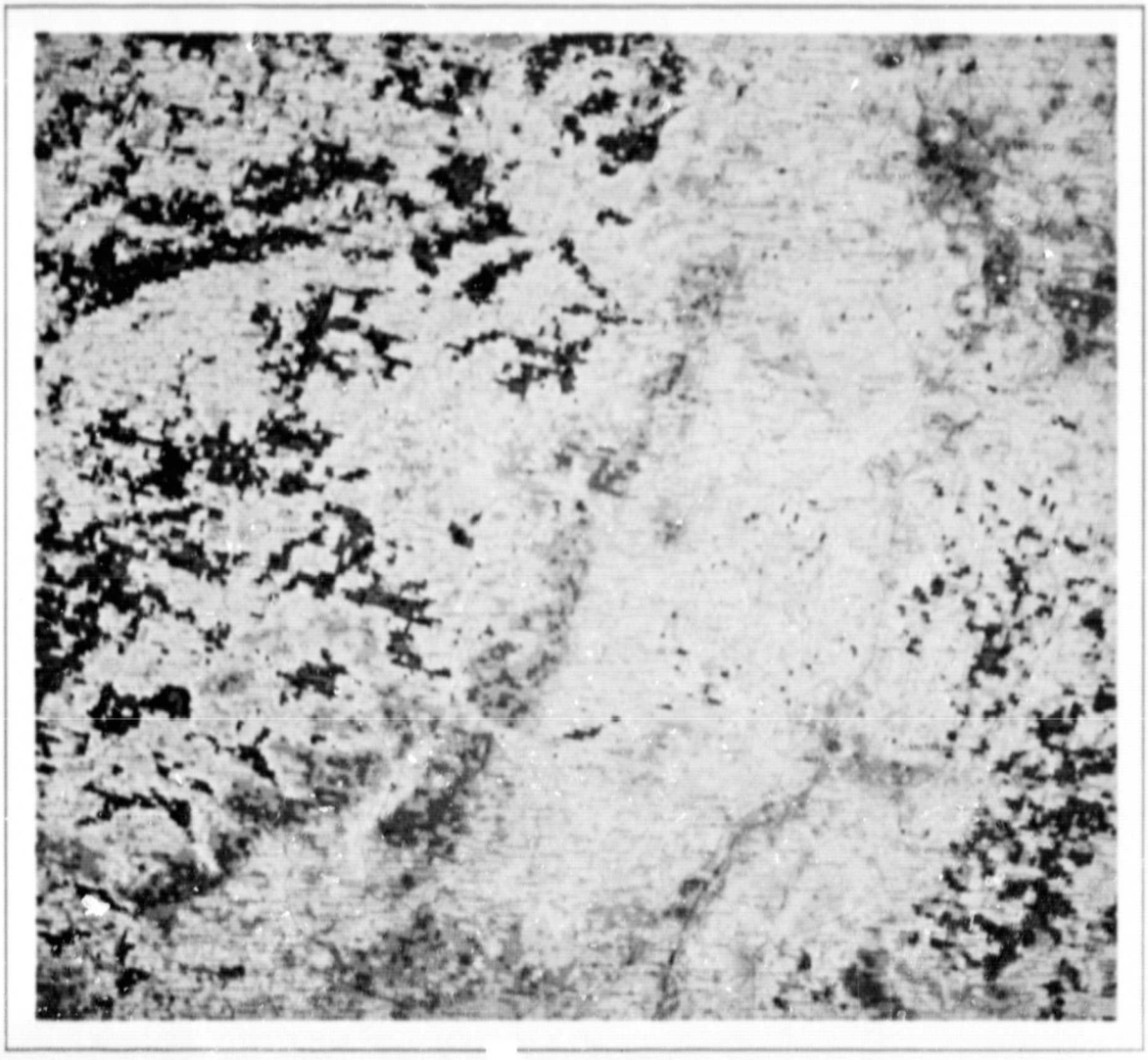

Fig. 10: Thermal-image (a section of TUK 200, sheet CC 7110 Mannheim) after the second step in the rectification ("fine" rectification, third to the last line in Fig. 8a). The superimposed information is from a topographical map.

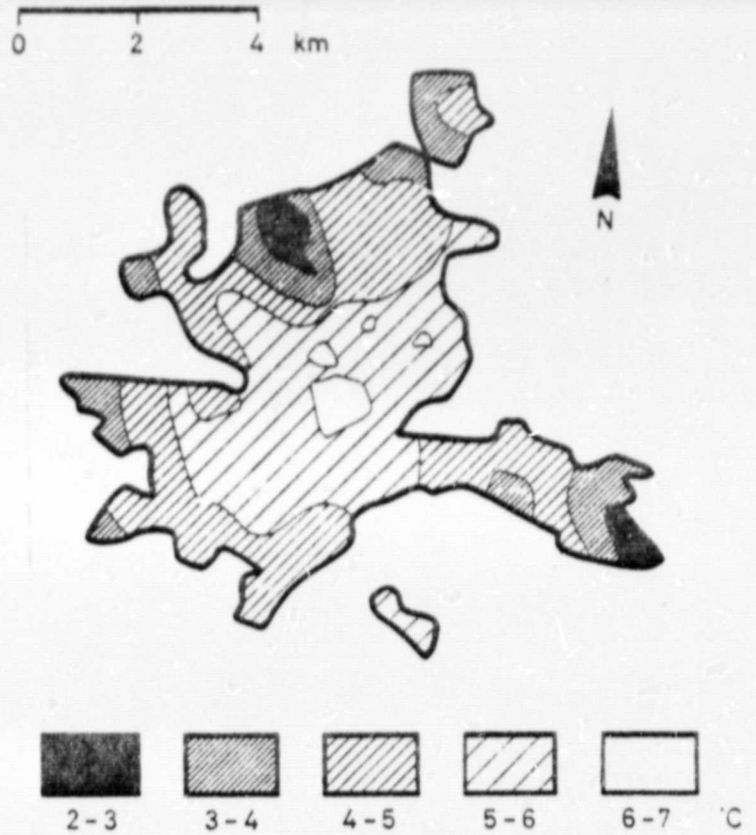

Fig. 11a: Surface-temperature distribution within the city of Freiburg on 5/30/79, 2:13 GMT (preliminary calibration), as revealed by the HCMM thermal-image following "fine" rectification and "smoothing" of the pixel edges.

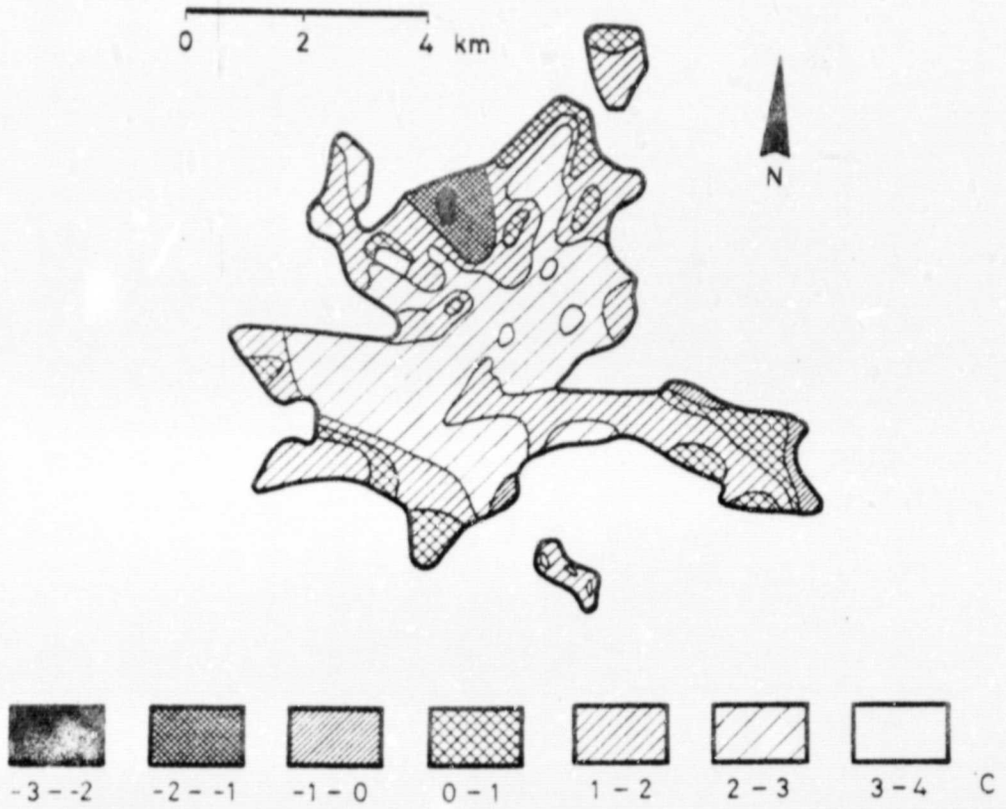

Fig. 11b: Surface-temperature distribution within Freiburg, taken from an aircraft scanner thermal image from 4/1/76 3:40 GMT, 4 000 m height above ground, resolution of the original pixels: 10 m.

4.2 Calibration, gray-level slicing, pseudocolour coding

The figures of this paper represent all HCMM-Data as temperature images in Celsius degrees. This has been used, because of better clearness, although the calibration of the data is not yet sure depending on several reasons:

- the effect of different emission capacity of the surface, which is not discussed here;
- the influence of the atmosphere on the recorded thermal data, and
- special problems of the NASA with regard to the calibration of the HCMM-data.

Since some characteristics of the HCMM sensor had changed after the launch, the internal calibration is not correct. Two experiments to get ground truth information in summer and autumn 1978 near White Sand in New-Mexico led to results which differed for about 5-6 degrees. Using the measurements of White Sands the original calibration procedure would result in values which are for images of May 1978 about 5.2 degress to high [6]. This error has been corrected of NASA when recording the CCT's (which was unknown to the authors) and during the evaluation, that means, at the present time to all temperatures of HCMM-images within this paper a constant of about 6 degrees has to be added.

For the reproduction of the temperature values in the DIBIAS system a "standardized" gray scale between 0 and 255 has been used with the following reference:

gray value	temperature
80	0°C
84	1°C
88	2°C
...	...
100	5°C
...	...

For the pseudocolour representation in Fig. 13 and 18 a 1-degree-scale with the following colour key has been used:

violett	-3 to -2°C		yellow/green	3 to 4°C	
dark blue	-2 to -1°C		yellow	4 to 5°C	
blue	-1 to 0°C		orange 1	5 to 6°C	
light blue	0 to 1°C		orange 2	6 to 7°C	
cyan	1 to 2°C		red	7 to 8°C	
green	2 to 3°C		dark red	8 to 9°C	

5. The construction of the multi-channel scene

As a result of the processing steps described above the following spatially correlated, digitized, and rectified image-information from the investigated area was derived:

- the HCMM-night-infrared-image-data with calibrated gray values;
- the HCMM-night-infrared-image-data with calibrated gray values which were also adapted to the temperature pseudo-colour-scheme;
- the network of urban built-ups;
- the forest distribution;
- the relief for the area represented in map CC 7110
- and the classified image data described in section 2.

By means of the ME-module (Merge-Modul, cf. [5]) the individual scenes have been transformed into two multi-channel scenes: one for the entire area under investigation and a second for the region represented in CC 7110.

The content of the various channels in the first multi-channel scene is sketched in Fig. 12a.

A pixel g of this scene is thus a vector in six dimensions $(g_1, g_2, g_3, g_4, g_5, g_6)$; the vector components correspond to the following categories:

g_1: = 230 elevation 0 - 200 m
= 180 " 200 - 400 m
= 130 " 400 - 700 m
= 80 " 700 - 1000 m
= 30 " > 1000 m

g_2: = 0 urban built-up
= 255 no urban built-up

g_3: = 0 forest
= 255 no forest

g_4: = 0 body of water
= 255 no body of water

g_5: $0 \leq g_5 \leq 255$ HCMM-night-IR-data, calibrated

g_6: $0 \leq g_6 \leq 255$ HCMM-night-IR-data, calibrated and adapted to the temperature pseudo-colour-scheme.

The second multi-channel scene overlays a portion of the map CC 7110. It was produced in a procedure similar to the one described above and consists of the following eight channels:

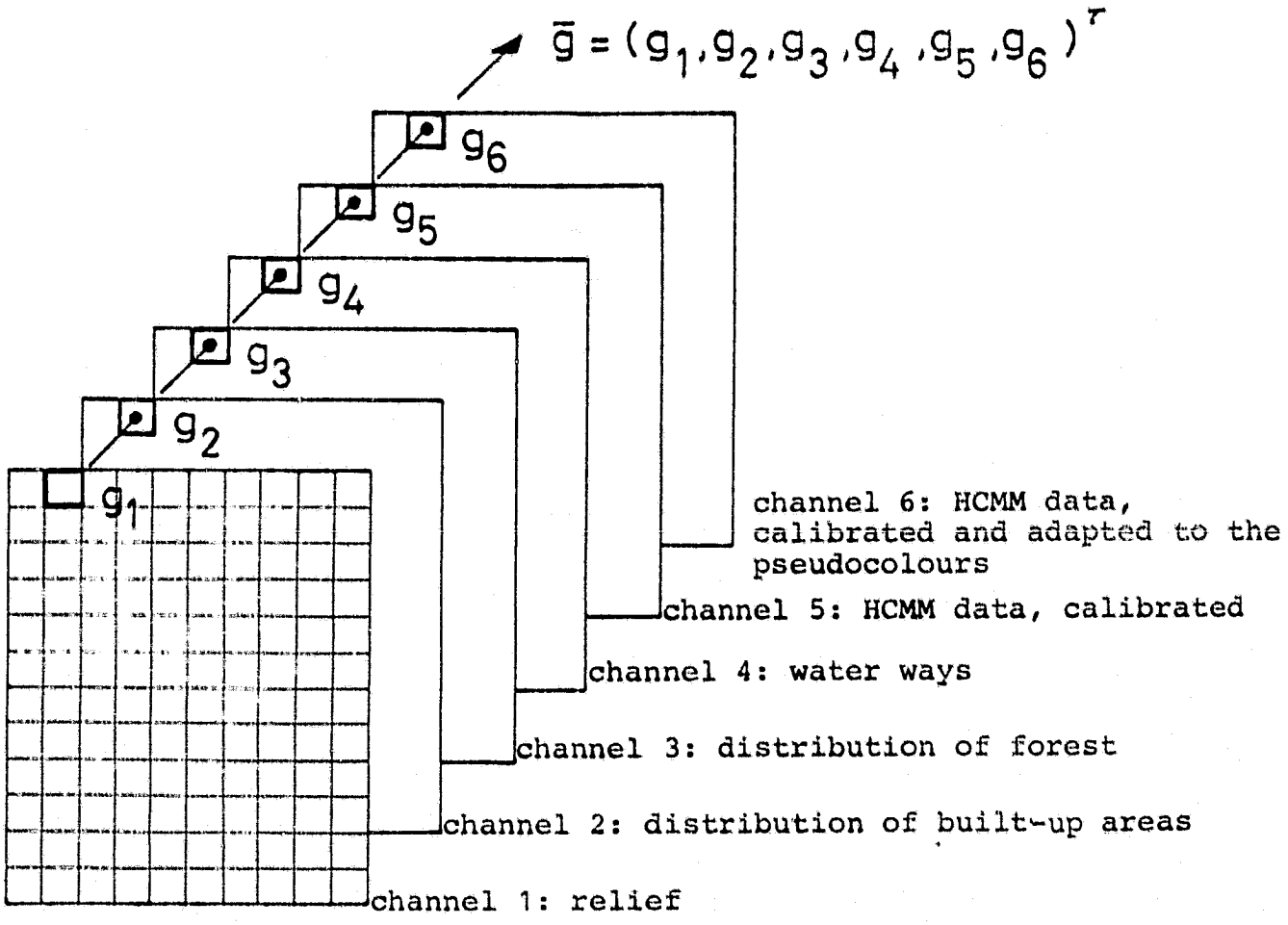

Fig. 12a: Data structure of the multi-channel scene for the whole area under investigation.

K_1 LANDSAT classification according to section 2.

K_2 HCMM-night-IR data, calibrated.

K_3 HCMM-night-IR data, calibrated and adapted to the temperature pseudo-colour-scheme.

K_4 HCMM-night-IR data, calibrated, averaged, and adapted to the temperature pseudo-colour scheme.

K_5 relief

K_6 urban built-up

K_7 water-ways

K_8 forest distribution.

6. Examples of evaluation

The data structures described in chapter 5 allow the combination of the different channels with their special information. A diversity of questions can be investigated with respect to the dependence of the surface temperature on other surface characteristics. Thus these data structures are useful aids for the investigation of the "thermal conditions of different parts of the landscape" [2]. In the following some examples of evaluation will be presented.

6.1 Surface temperature and relief

Fig. 6 demonstrates already that the relief of a landscape is reflected in thermal infrared images recorded at night, that means, that the relief has an essential influence on the surface temperature. One possibility to investigate this correlation is the extraction of the thermal data for several elevation levels of the thermal image. The thermal images of the different elevation levels produced by this procedure (Fig. 13) demonstrate what kind of parameters influence the surface temperatures. Thus the highest surface temperatures (without consideration of the large cities) do not occur in the Rhine Valley (0 - 200 m) but at the slopes of the highlands. These are in the northern part of the Rhine Valley mainly the regions between 200 and 400 m and in the southern part those between 400 and 700 m. Very warm are isolated elevations between 400 and 700 m, e.g. in the northern part of the Voges montains. Relatively high however, are the temperatures of the Rhine Valley in comparison to the plains of the highlands, e.g. in the region east of the Black Forest. In the great shallow depressions which can be found there in about 700 m, occur the lowest surface temperatures of south-west Germany. This discussion could be continued, but the above mentioned hints demonstrate already, that the thermal images of different elevation levels can be used in order to investigate how the altitude of the surface and how the relief of its environment will have an influence on the temperature of the surface at night.

0 —
200 m

200 —
400 m

400 —
700 m

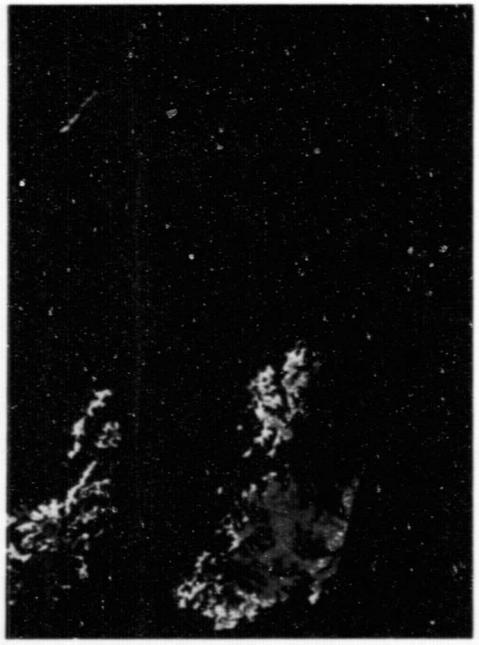

700 —
1000 m

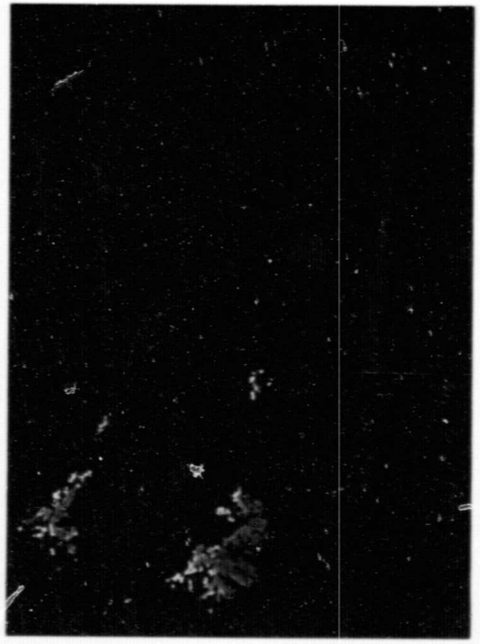

> 1000 m

Fig. 13: Surface temperatures at different elevations of the investigated area as recorded 5/30/78 by the HCMM satellite (preliminary calibration) red ≙ warm; blue ≙ cold. 1-degree-levels: cyan/green 2° C.

6.2 Surface temperature and land-use

Besides the relief, different land use types will be reproduced in the thermal image, depending on their individual heat budget. Thus in Fig. 6 the cities of Basel, Strasbourg, Mannheim and Frankfurt appear as warm areas, similar to extended forest areas in the Rhine Valley or in the highlands. Using this fact, the data structures can be used to separate individual land-use types and to quantify the influence of the special type of land-use on the surface temperature. For the region of the topographical map CC 7110 (1:2,000,000, Mannheim), for which the Landsat derived land-use classification has been integrated into the data structure, statistics of the surface temperature for each land-use type can be calculated. Without regarding the influence of the relief, this evaluation has been calculated for the elevation level 0 - 200 m, according to the elevation of the Rhine valley (Fig. 15). The gray values 90, 100 and 110 of the abscisse in Fig. 15 correspond to the temperatures 2.5, 5 and 7.5 °C. For the better understanding of the evident correlation of the surface temperature with the type of landuse, the whole region of CC 7110 has been overlaid with a grid of 5 x 5 km^2 (Fig. 16). For each of these squares the distribution of the different land-use classes can be calculated. Fig. 17 is an example of this calculation for four of these squares, containing the distribution of the classification, the parts of built-up and forest areas derived from the digitized maps and the mean surface temperature of the HCMM data. The values demonstrate, that high surface temperature coincides with large portions of built-up areas and that low surface temperature coincides with large portions of agricultural land. On the other hand the question arises, why the large area of forest in square No. 3 (Bienwald) does not produce high temperatures. To investigate these problems more carefully, the data of the nearly 150 squares will be evaluated with a regression analysis.

6.3 Surface temperature and built-up areas

Of special economical interest are the patterns of the surface temperature of the built-up areas. At the beginning it was unknown whether the resolution of 600 m of the HCMM satellite was sufficient for the recording of certain built-up areas, the determination of the thermal structures in highly populated regions and the comparison of different built-up areas. Fig. 11a demonstrated already, that the HCMM image, with the impact of geometrical rectification, allows a correct overview of the city of Freiburg im Breisgau. Fig. 18 is an example of a survey over the surface temperature of all built-up areas within CC 7110, using an appropriate subset data structure derived from the Landsat classification. This example contains the surface temperature derived from the HCMM-image and the cities and inner city regions of the Landsat classification, thus giving an overview of the large cities (Mannheim/Ludwigshafen, Karlsruhe, Kaiserslautern) and permits a comparison of the temperature of cities of the same area and their environment.

Fig. 14: Land use map of TUK 200 CC 7110 (Mannheim) derived from Landsat data. The image shows the results of the classification with an overlay of the topographic map. Meaning of colours: dark red - city; red - mixed urban or built-up land; light green - orchards and pasture; yellow - agricultural land; violet - vineyards; blue - water; dark green - coniferous forest; and green - deciduous forest.

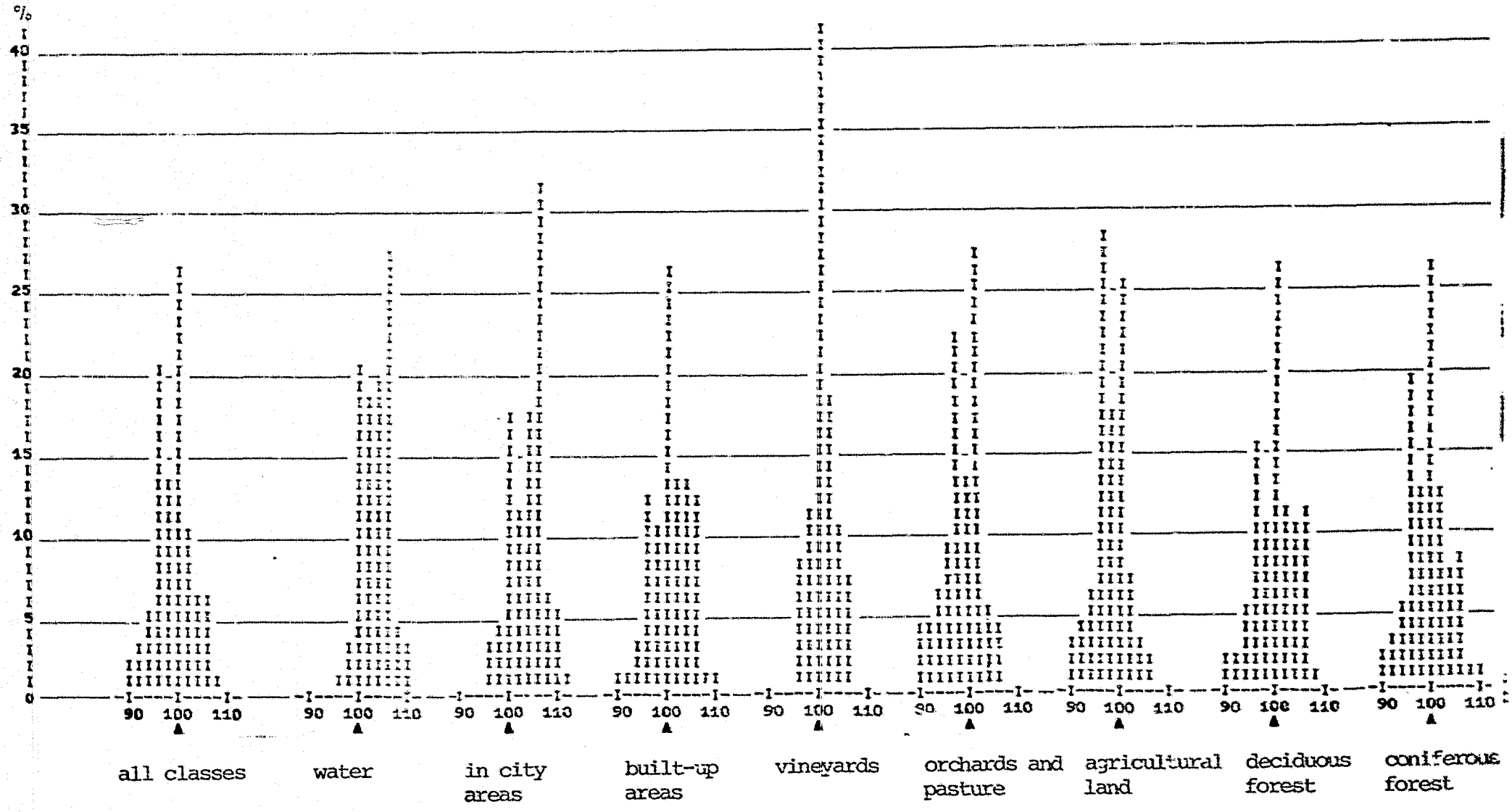

Fig. 15: Temperature-histogram of all surfaces less than 200 m in elevation in the region of the TÜK 200 CC 7110 (Mannheim). Land-use classes as in Fig. 14.

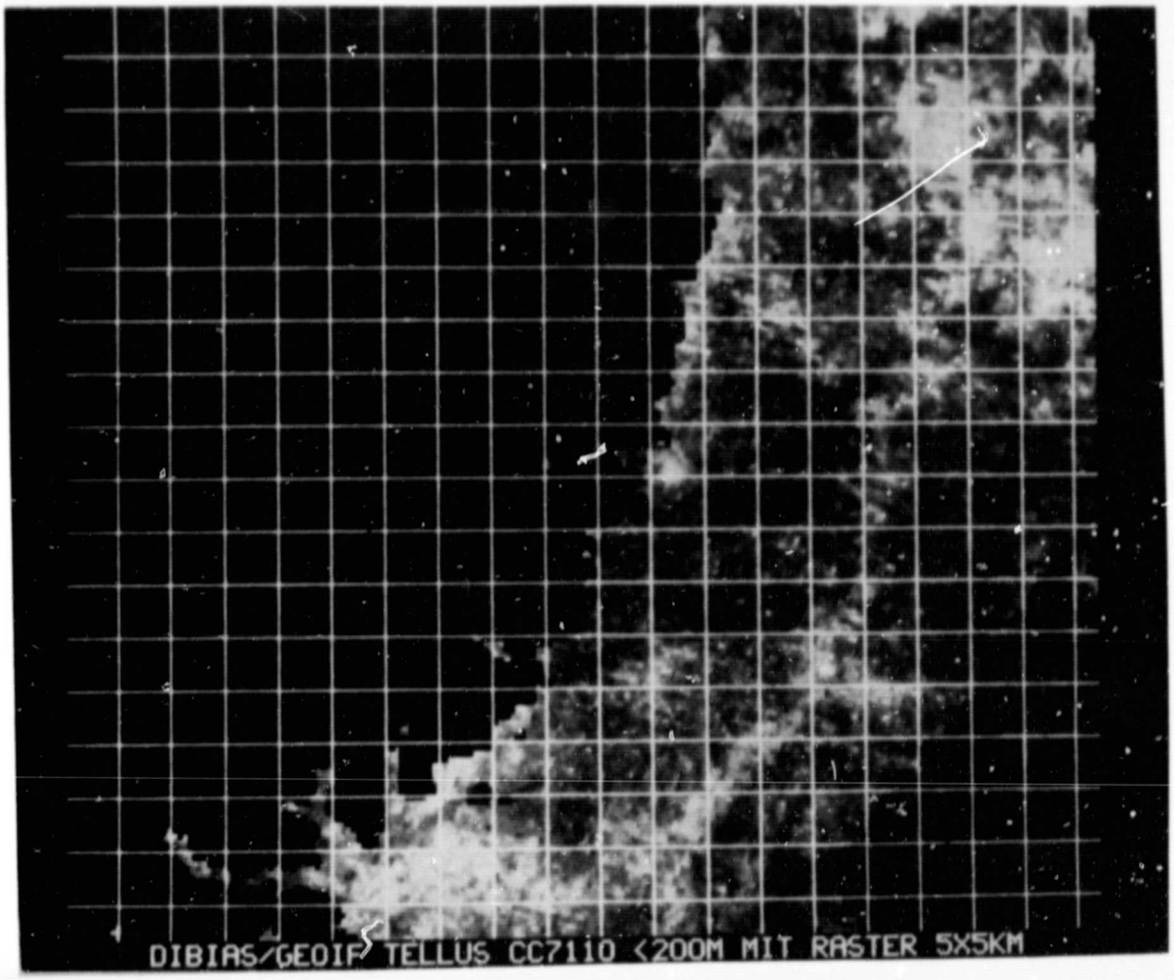

Fig. 16: This figure represents temperatures of all surfaces with elevations of less than 200 m in the region of CC 7110 (Mannheim).
Grid-distance 5 km. This will be used in order to derive the correlation between the average surface temperature of a square element of landscape and the relative distribution of the land-use classes within this square.

35

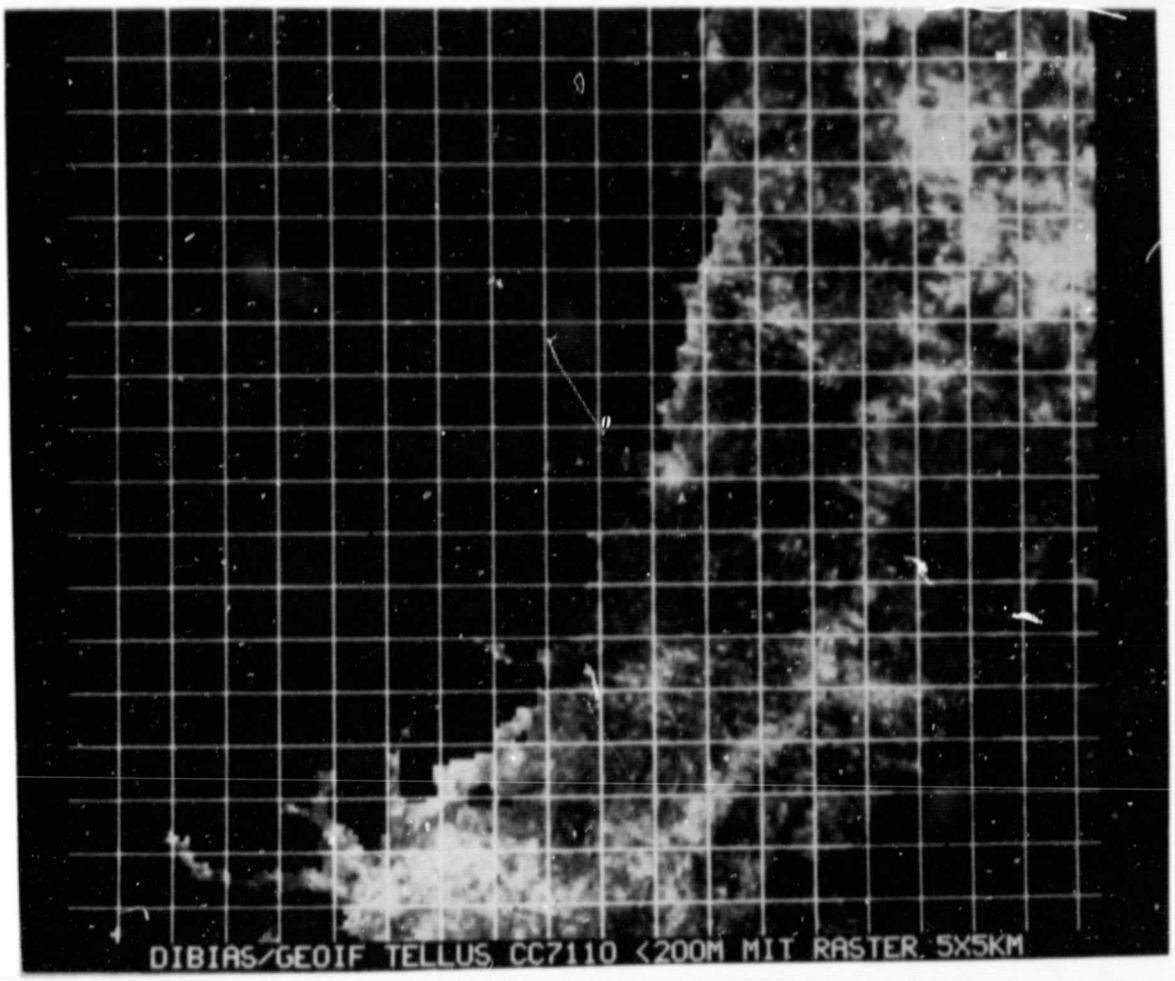

Fig. 16: This figure represents temperatures of all surfaces with elevations of less than 200 m in the region of CC 7110 (Mannheim).
Grid-distance 5 km. This will be used in order to derive the correlation between the average surface temperature of a square element of landscape and the relative distribution of the land-use classes within this square.

	Land-use type derived from the Landsat-classification							Land-use type derived from the thematic maps		Mean surface temperature (HCMM)	
	urban built-ups	city centres	agricultural land	orchards and pasture	vineyards	coniferous forest	deciduous forest / water	built-up areas	forest	mean gray value	preliminary calibration
Square 1 (Bad Dürkheim)	22%	–	12%	6%	56%	2%	2%	20%	4%	100.8	5.2 °C
Square 2 (Mannheim)	28%	68%	–	–	–	–	– 4%	98%	–	106.4	6.6 °C
Square 3 (Bienwald)	–	–	–	20%	–	22%	58% –	–	86%	99.5	4.9 °C
Square 4 (Schifferstadt)	3%	–	90%	7%	–	–	– –	4%	–	97.3	4.3 °C

Fig. 17: Surface temperatures and relative distribution of land-use classes in various grid quadrants of the Upper Rhine Plain in the area of Mannheim.

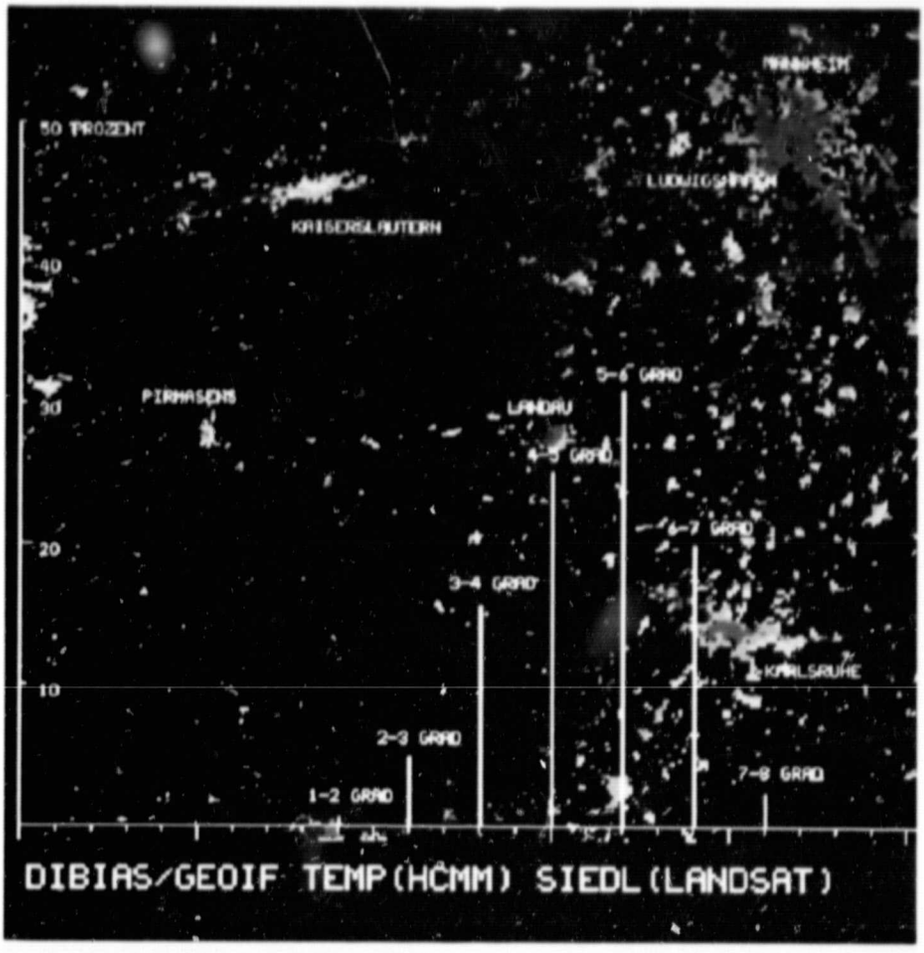

Fig. 18: Surface-temperatures (preliminary calibration) of built-up areas in the region of CC 7110 (Mannheim). The built-up areas correspond to the land-use classification derived from LANDSAT data (Fig. 14). The overlaid histogram (white) shows the fractional portions of the individual 1-degree-levels with respect to the entire temperature range of the built-up areas.

7. Conclusions

The evaluation of the described data structure is not complete with the presented examples, however, the investigations described in this paper demostrate:

- which accuracy can be achieved for the geometrical rectification of HCMM-data onto the coordinate system of topographical maps;
- that it is useful to correlate the rectified HCMM-data with other information , e.g. thematic maps of preprocessed Landsat-data.

The examples presented for the geometrical rectification of HCMM-data with an r.m.s. error of less than one pixel are, in our opinion, the best that can be achieved with the algorithms used. Better results could be obtained with the digitizing of the maps, if devices existed which allow scanning without a reduction in the size of the maps and without the photographic discrimination of the gray levels.

The investigation of the heat budget of several landscape types, which is the background aspect, may be extended in two directions:

- HCMM images of several recording dates, preferably images of day and night of the same date, must be included in the data structure, as soon as they are available.
- Maps of the air temperature distribution for the dates of image recording should be integrated into the data structure.

The knowledge of the daily amplitude of the surface temperature and the differences to the temperature of the air (the correct calibration presumed) would allow the investigation of regional heat budgets.

8. References

[1]	NASA:	Heat Capacity Mapping Mission (HCMM) Data Users Handbook for Applications Explorer Mission-A (AEM).
[2]	GOSSMANN, H.	The thermal behaviour of natural and cultural landscape regions in southern Germany as derived from satellite imagery. Publication in preparation; 1980.
[3]	SCHIKARSKY, W. et al.	Das Abwärmeprojekt Oberrheingebiet - Aufgaben und Ziele. Bericht des Kernforschungszentrums Karlsruhe, Laboratorium für Aerosolphysik I, März 1977.
[4]	HABERÄCKER, P. et al.	Auswertung von Satellitenaufnahmen für die Landnutzung. Schriftenreihe "Raumordnung" des Bundesministers für Raumordnung, Bauwesen und Städtebau, Bonn 1980.
[5]	FERNANDEZ, S. et al.	DIBIAS-Handbuch DFVLR, Institut für Nachrichtentechnik, Oberpfaffenhofen 1976.

ERRATUM

The numbers of pages 33 and 37 have been exchanged:

Fig. 14 should be on page 33
Fig. 18 should be on page 37